ELECTRON DISTRIBUTION FUNCTIONS ASSOCIATED WITH ELECTROSTATIC EMISSIONS IN THE DAYSIDE MAGNETOSPHERE

by

D.D. Sentman,

Institute of Geophysics and Planetary Physics, University of California, Los Angeles, CA 90024

L.A. Frank, D.A. Gurnett, and W.S. Kurth

Department of Physics and Astronomy, University of Iowa, Iowa City, IA 52242

C.F. Kennel,

Department of Physics, Center for Plasma Physics and Fusion Engineering, and Institute of Geophysics and Planetary Physics, University of California, Los Angeles, CA 90024

Abstract. Electron distribution functions constructed from ISEE-1 dayside observations of low energy magnetospheric electrons at low latitudes are presented. We choose examples corresponding to three distinct types of odd half harmonic electrostatic emissions observed by the plasma wave experiment on ISEE-1, and occurring between the electron cyclotron frequency f_{ce} and the upper hybrid frequency f_{UH}. These are (a) intense $(3/2)f_{ce}$ emissions; (b) weak $(n + 1/2)f_{ce}$ noise; and (c) intense f_{UH} waves at $(9/2)f_{ce}$. No loss cone-like features are discernable in any of the distribution functions at the level of the instrument angular resolution. However, a weak ringlike feature, consisting of a small localized region in velocity space near 4×10^9 cm s^{-1} and $\alpha = 90^o$ where $\partial f/\partial v_\perp > 0$, is found in the distribution function corresponding to the occurrence of the intense f_{UH} noise. This ringlike feature may provide a source of free energy to drive the f_{UH} instability. The apparent absence of detectable loss cones in the cases of the intense $(3/2)f_{ce}$ and f_{UH} emissions is consistent with the expectation that these plasmas are roughly at the level of strong pitch angle diffusion computed from the observed wave intensities at these times. Although each of the distribution functions displays a temperature anisotropy $T_\perp > T_\parallel$, the anisotropies are too small to excite any of the odd half harmonic emissions.

Introduction

Recent advances in spacecraft instrumentation for measuring charged particle distribution functions and plasma wave spectrums in the magnetosphere have made possible detailed comparative studies between observations and microscopic plasma theory. A topic of recent interest has been an observational test of the theoretical requirements for the generation and maintenance of banded electrostatic emissions at odd-half harmonics of the electron gyrofrequency f_{ce} in magnetospheric plasmas. These emissions in various forms pervade the magnetosphere and are thought to cause the precipitation of few keV electrons responsible for the diffuse aurora [*Kennel et al.*, 1970; *Lyons*, 1974].

The theoretical elucidation of the electrostatic instability leading to the observed plasma emissions has been based on models of the electron distribution function consisting of a cold component (few eV), presumably of ionospheric origin, and a hot component (few keV) of plasma sheet origin [*Young et al.*, 1973; *Ashour-Abdalla and Kennel*, 1976, 1978; *Hubbard and Birmingham*, 1978]. In these models, a $\partial f/\partial v_\perp > 0$ loss cone feature in the hot component provides the free energy to drive the instability, while the cold component strongly influences phase and group velocities. Plasma observations relating the parameters of the hot and cold components of the electron distribution function to spectral characteristics of the banded electrostatic emissions have recently been reported by *Christiansen et al.* [1978], and *Hubbard et al.* [1979].

In the present work we present some preliminary results of an analysis of ISEE-1 low energy electron data 230 eV $< E_e <$ 45 keV obtained from a quadrispherical Lepedea [*Frank et al.*, 1978a] during a single inbound pass through the low latitude magnetosphere near local noon. Three distinct types of odd-half harmonic electrostatic emissions were observed between f_{ce} and the upper hybrid frequency f_{UH} [*Gurnett et al.*, 1979]: (a) intense, narrow band emissions at roughly $(3/2)f_{ce}$ [*Kennel et al.*, 1970]; (b) spectrally diffuse, low intensity waves with peak intensities near $(n + 1/2)f_{ce}$ [*Shaw and Gurnett*, 1975]; and (c) intense, narrow band emission at f_{UH} near $(9/2)f_{ce}$ [*Kurth et al.*, 1979a]. We present power density spectrums of each of the respective emissions together with the corresponding electron distribution functions $f(v_\perp, v_\parallel)$. We parameterize the electron distributions, attempt to identify possible sources of free energy, and discuss structural differences in the light of quasilinear diffusion rates based upon the observed wave amplitude spectrums.

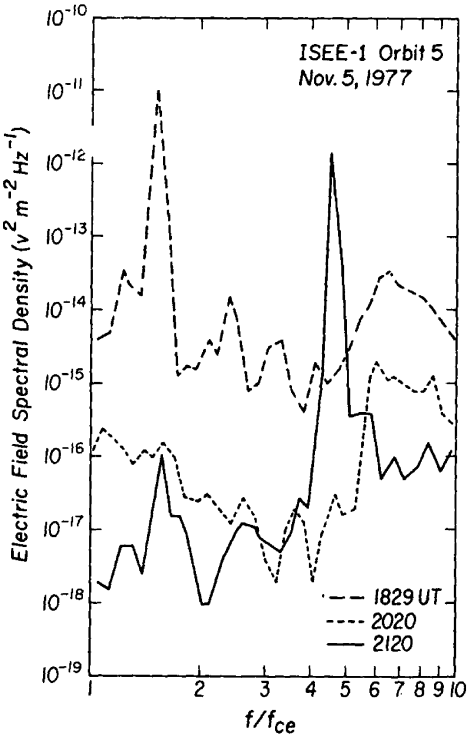

Figure 1. Spectral densities of electrostatic emissions averaged over eight-minute intervals centered on the indicated times. The three curves are for (a) intense narrow band $(3/2)f_{ce}$ waves at 1829 UT; (b) low intensity diffuse noise centered on 2020 UT peaking roughly at $(n + 1/2)$ f_{ce} in the frequency interval $f_{ce} < f < f5_{ce}$; and (c) an intense burst of very narrow band f_{UH} waves near $(9/2)f_{ce}$ centered on 2020 UT. The curve for (c) does not include the actual peak of the most intense 7 mV/m burst, since this was sufficient to saturate the receiver and preclude accurate determination of the spectral density.

Paper number 9L1223.
0094-8276/79/009L-1223$01.00

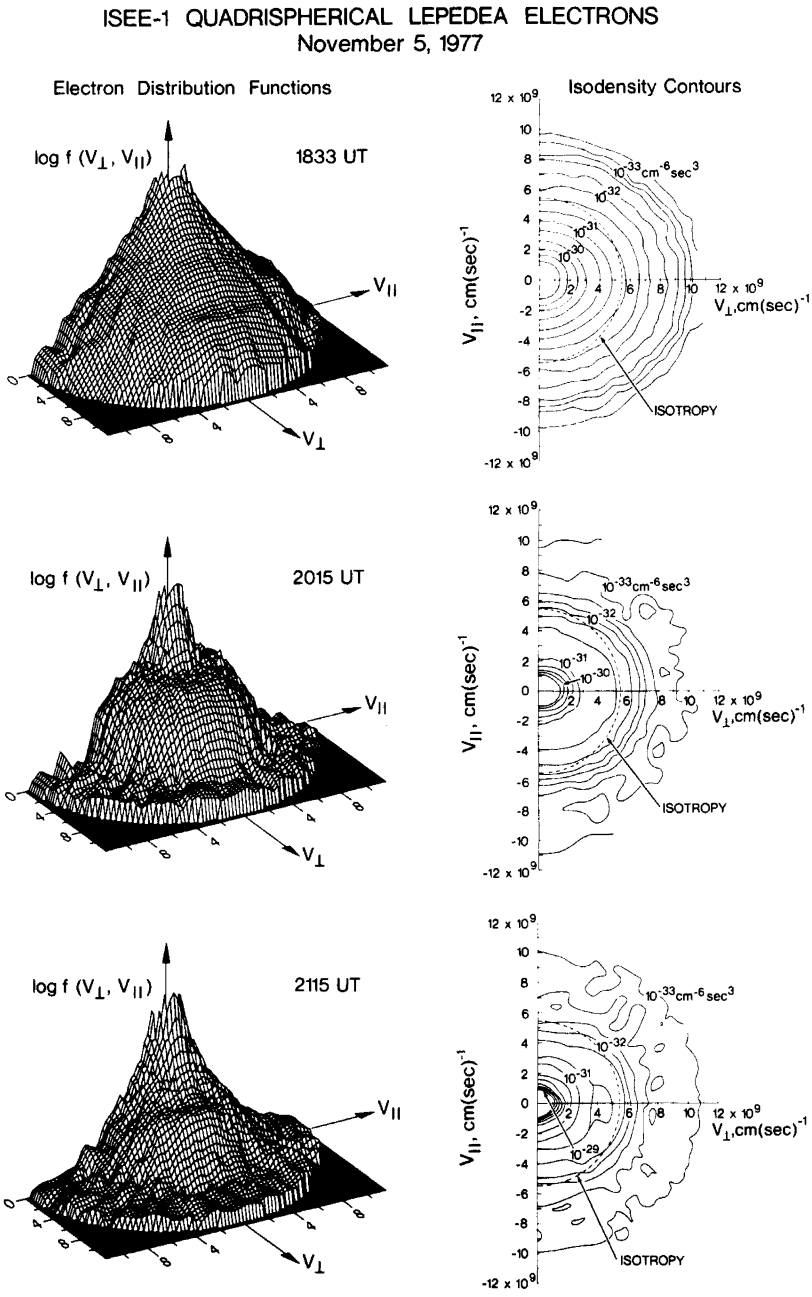

Figure 2. Distribution functions $f(v_\perp, v_\parallel)$ of electrons in the energy range 230 eV $\leq E_e \leq$ 45 keV. The orthogonal hidden line projections of the $f(v_\perp, v_\parallel)$ surfaces are onto a screen normal to a line passing through the origin and of 15° elevation above the $(v_\perp, v_\parallel)$ plane and azimuth 330° measured counterclockwise from the $v_\perp$ - axis, and were produced at UCLA. The corresponding isodensity contour plots on the right have three logarithmically spaced contours per decade, labeled at integer values of log $f(v_\perp, v_\parallel)$, and were produced at the University of Iowa.

Data Selection and Results

Time periods for selection of ISEE-1 low energy electron data were determined by scanning high resolution spectrograms from the plasma wave instrument aboard the same spacecraft [*Gurnett et al.*, 1978]. During a Nov. 5, 1977 inbound pass, ISEE-1 penetrated the magnetopause at 1720 UT near local noon and at roughly 20° N geomagnetic latitude. Sporadic bursts of both $(3/2)f_{ce}$ waves and odd half harmonic emissions were observed to occur with varying degrees of persistence and intensities until about 1900 UT. At this time the $(3/2)f_{ce}$ waves ceased simultaneously with a decrease in the intensities of electrons $E_e > 230$ eV observed with Lepedea. Between the 1720 UT magnetopause crossing and 1900 UT the onboard magnetometer also recorded magnetic intensity fluctuations with 1–10 min time scales at roughly the ten percent level (C.T. Russell, private communication, 1979). A period of sustained (3/2) f_{ce} activity with amplitudes of 0.1–1 mV/m occurred from 1825-1837 UT. From 1900 UT until approximately 2030 UT the plasma wave data in the frequency range $f_{ce} < f < f_{UH}$ were dominated by the low intensity diffuse electrostatic waves near $(n + 1/2)f_{ce}$. From 2030 UT until the spacecraft crossed the plasmapause at about 2125 UT, the dominant wave activity was in a narrow band of frequencies about f_{UH}. Within this time period, from approximately 2108 UT until 2118 UT, an intense burst of upper hybrid noise occurred, with peak amplitudes of 7 mV/m, as reported by *Gurnett et al.* [1979]. We have therefore calculated electron distribution functions derived from electron data taken in the intervals 1829-1837 UT, 2011-2019 UT and 2111-2119 UT corresponding to the three different types of electrostatic wave activity. Spectral densities of these waves from periods overlapping these particle accumulation intervals are shown in Figure 1. Interested readers may find an intensity-time spectrogram for the interval 1830-2230 UT on this day (Nov. 5, 1977) and a discussion of its interpretation in *Kurth et al.* [1979b].

Frank et al. [1978a,b] have given a complete description of the quad-

rispherical Lepedea. On Nov. 5, 1977 during the period 1927-2125 UT, the Lepedea was in a mode that scanned the energy range 230 eV - 45 keV in 32 logarithmically spaced energy steps. Energy resolution was 17% and the energy scan cycle required about eight minutes to complete. The average pitch angle resolution was about 15°. Figure 2 shows the electron distribution functions $f(v_\perp, v_\parallel)$ over the energy range 230 eV - 45 keV for our three selected time intervals. The perspective plots on the left are two-dimensional orthogonal projections of the three-dimensional log $f(v_\perp, v_\parallel)$ surfaces; the plots on the right are the equivalent isodensity contour plots.

To facilitate quantitative comparisons, it is convenient to characterize the number densities, temperatures and anisotropies of the distribution functions of Figure 2. A nonlinear least squares fit was made to each example for $v < 8 \times 10^9$ cm-s^{-1} using a double bimaxwellian of the form $f = f_1 + f_2$, where

$$f_i = \frac{n_i}{\pi^{3/2} a_{i\perp}^2 a_{i\parallel}} \exp\left[-\left(\frac{v_\perp^2}{a_{i\perp}^2} + \frac{v_\parallel^2}{a_{i\parallel}^2}\right)\right], \quad i = 1,2,$$

$a_{i\perp}^2 = 2T_{i\perp}/m$, $a_{i\parallel}^2 = 2T_{i\parallel}/m$, m is the electron mass, $T_{i\perp}$ and $T_{i\parallel}$ are the respective perpendicular and parallel temperatures and n_i is the number density of component i. The results are tabulated in Table 1, along with the anisotropies $\Delta_i = (T_{\perp i}/T_{\parallel i} - 1)$ for each component, the total electron densities n_T computed from the lower cutoff frequency of the continuum radiation [*Gurnett et al.*, 1978], and relevant orbit parameters.

1833 UT: The electron distribution function observed in association with the intense $(3/2)f_{ce}$ emissions (top of Figure 2) displayed a monotonically decreasing, relatively smooth velocity spectrum. No persuasive evidence for a loss cone or other nonmonotonic feature such that $\partial f/\partial v_\perp > 0$ is observed. This does not preclude the existence of such features, however. A shallow loss cone, for example, could be present but not detectable due to the finite angular resolution of the instrument (see, e.g., *Kurth et al.* [1979a] for a discussion of this effect).

If we define the number density of the hot electrons to be $n_H = (n_1 + n_2)$, where n_1 and n_2 are from the least squares fits of Table 1, and the cold density n_c to be the difference between the total density n_T and n_H, then the cold to hot ratio n_c/n_H for this case is roughly 4. The temperature anisotropy Δ_2 of the hotter of the two components is approximately 0.4, while that of the cooler component, Δ_1, is only 0.04. These temperature anisotropies are too small to excite the $(3/2)f_{ce}$ instability [*Ashour-Abdalla and Kennel*, 1978] to produce the observed emissions. A candidate source of free energy to drive this instability has therefore not been identified in the present example.

2015 UT: During the time period when the diffuse $(n + 1/2)f_{ce}$ banded noise dominated, the distribution function $f(v_\perp, v_\parallel)$ consisted of three distinct populations (middle of Figure 2). The low energy peak corresponds to a population of electrons with a number density n_1 of about 0.07 cm^{-3} and temperature of 100 eV (see Table 1). The corresponding anisotropy is 0.75. The intermediate component has a number density $n_2 \sim 0.05$, and temperature $T_2 \sim 4$-5 keV; the temperature anisotropy $\Delta_2 \sim 0.8$. The cold to hot ratio in this case is $n_c/n_H \sim 15$. Beyond 8-9 x 10^9 cm-s^{-1} the distribution flattens into the beginning of the energetic electron spectrum. No persuas evidence of a loss cone or other nonmonotonic feature is present, although a relatively broad plateau of nearly constant slope $\partial f/\partial v$ exists near velocities of 4 x 10^9 cm-s^{-1}. Detailed analysis of this plateau shows that $\partial f/\partial v_\perp$ is weakly negative over its domain.

Table 1. Electron Distribution Function Model Parameters

77 Nov. 5, UT	1833	2015	2115
Type waves	3/2 f_{ce}	(n+1/2)f_{ce}	UH
R/R_E	10.0	7.3	5.4
LT	1145	1211	1244
λm	18.7	12.1	6.6
n_T, cm^{-3}	1.1	2.0	6.7
f_{pe}/f_{ce}	6.2	5.0	4.2
n_1, cm^{-3}	0.094	0.074	0.18
$T_{1\perp}$, eV	250	140	130
$T_{1\parallel}$, eV	240	80	100
Δ_1	0.04	0.75	0.30
n_2, cm^{-3}	0.12	0.05	0.04
$T_{2\perp}$, keV	3.4	5.7	4.1
$T_{2\parallel}$, keV	2.5	3.2	3.6
Δ_2	0.40	0.80	0.14
n_c/n_H	4.1	15	30

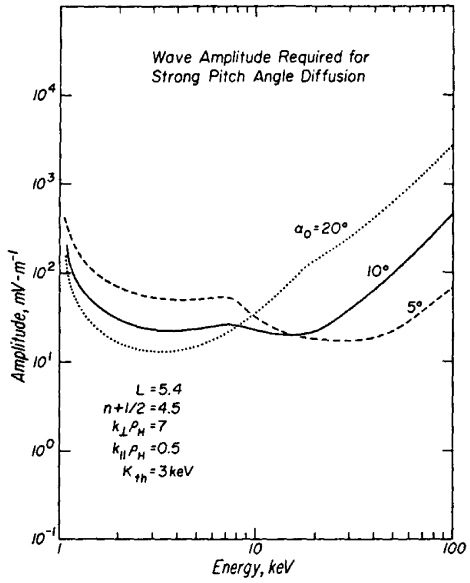

Figure 3. Wave amplitudes of narrow band waves required to pitch angle diffuse an electron an angle equal to its equatorial pitch angle α_o in a quarter bounce period. The wave spectrum assumed is of an analytical form similar to that of *Lyons* [1974], with the wave energy peaked at $(9/2)f_{ce}$, $k_\perp\rho_H = 7$ and $k_\parallel\rho_H = 0.5$, where $k_\perp$ and $k_\parallel$ are the respective perpendicular and parallel wavenumbers, and ρ_H is the hot electron thermal gyroradius. The plasma thermal energy is assumed to be 3 keV, and the waves to be uniformly distributed in amplitude along a field line labeled L = 5.4. Similar calculations for a narrow band spectrum at (3/2) f_{ce}, assuming a wave spectrum peaked at $k_\perp\rho_H = 2$, $k_\parallel\rho_H = 0.5$ located at L = 10, indicate that wave amplitudes of 0.5 – 1 mV/m are required in this case to put the plasma on strong diffusion at energies greater than several keV.

2115 UT: The electron distribution function observed during the period of intense UH noise is shown in the bottom of Figure 2. The overall structure is reminiscent of the previous example, in that a low energy component and a high energy tail are observed. A component of intermediate temperature is also present. The relatively broad plateau of the previous example has been reduced in size to a small region centered near 4 x 10^9 cm-s^{-1} and pitch angle $\alpha = 90°$. Detailed analysis of this plateau region reveals that the slope $\partial f/\partial v_\perp$ is weakly positive [*Kurth et al.*, 1979a], as is explicitly shown in the contour plot for this time period. Thus a potential free energy source is available from this weak ringlike distribution (referred to as a "bump on tail" by *Kurth et al.* [1979a]) for driving the accompanying intense UH noise. The cold to hot ratio n_c/n_H is roughly 30, and the temperature anisotropy has decreased relative to the previous case; $\Delta_1 \sim 0.3$ and $\Delta_2 \sim 0.14$. No persuasive evidence for a loss cone is observed at this time.

Discussion

The distinct two-component form of the distribution functions at 2015 UT and 2115 UT at velocities $v \leqslant 8 \times 10^9$ cm/s is similar to that reported both near the inner edge of the plasma sheet near local midnight [*Schield and Frank*, 1970] and at low altitudes equatorward of the dayside auroral oval [*Craven and Frank*, 1976]. In each of the cited studies,

the energy of separation between the two populations was 1-2 keV, which is comparable to the present case. As in *Craven and Frank* [1976], a possible interpretation of the present two component form, exclusive of the high energy tail, is that these electrons are of plasma sheet origin and have convected around the dawnside of the earth to their observed locations.

The absence in our data of a discernable loss cone at 1833 UT raises the question of the free energy source driving the intense $(3/2)f_{ce}$ emissions observed at this time. However, if the instability is nonconvective, relatively small and obscure features in the distribution function could produce large local wave amplification [*Ashour-Abdalla and Kennel*, 1978]. Inspection of a high time resolution frequency-time spectrogram for the period 1800-1900 UT reveals that the frequency of maximum wave intensity near $(3/2)f_{ce}$ tracks the magnetic fluctuations occurring during this time period. This correlation suggests that the $(3/2)f_{ce}$ emissions under consideration may indeed be produced and amplified locally and nonconvectively.

The relative "smearing" between the two populations n_1 and n_2 when either intense $(3/2)f_{ce}$ of f_{UH} noise is present (top and bottom of Figure 1), compared to when the weak $(n + 1/2)f_{ce}$ noise dominates (middle of Figure 2), may be the result of quasilinear diffusion of electrons [*Kennel and Engelmann*, 1966; *Scarf et al.*, 1973]. In order to test the possibility that the $(3/2)f_{ce}$ and f_{UH} waves are sufficiently intense to put the plasma on strong pitch angle diffusion, we have explicitly calculated the quasilinear pitch angle diffusion coefficients for each case separately. Figure 3 shows, as a function of energy, the approximate wave amplitudes required to put the thermal plasma associated with the upper hybrid noise on strong pitch angle diffusion. We analytically modeled the upper hybrid noise spectrum after *Lyons'* [1974] model for $(3/2)f_{ce}$ noise (see caption for Figure 3 for model parameters). The observed 7 mV/m amplitude of these waves is close to the required ~10 mV/m, indicating that the plasma may be nearly in a state of strong pitch angle diffusion. Similar calculations for the $(3/2)f_{ce}$ case yield ~0.5-1 mV/m for the amplitude of the waves needed to put the plasma at 1833 UT on strong pitch angle diffusion. These wave amplitudes are also roughly at the level of those observed.

Summary and Conclusions

In this preliminary report we have examined distribution functions $f(v_\perp, v_\parallel)$ of electrons 230 eV $\leq E_e \leq$ 45 keV associated with three distinct types of electrostatic emissions occurring in the low latitude dayside magnetosphere. A feature common to each of the distribution functions is a temperature anisotropy $T_\perp > T_\parallel$. We find the temperature anisotropies associated with the intense $(3/2)f_{ce}$ and f_{UH} emissions to be too small ($\leq$0.5) to excite either of these instabilities. Although none of the distribution functions display a discernable loss cone-like structure, shallow loss cones could still be present but not detectable due to the finite angular resolution of the instrument.

Detailed inspection of the distribution function occurring in association with the intense burst of f_{UH} noise near 2115 UT shows the existence of a small region in velocity space near $v \sim 4 \times 10^9$ cm/s and $\alpha = 90^o$ where $\partial f/\partial v_\perp > 0$. This ringlike distribution of particles, superimposed on a distribution function which is otherwise more or less monotonically decreasing with velocity, may provide the source of free energy required to drive the instability. Previous theoretical descriptions of f_{UH} noise have tended to rely on loss cone-like structures in the distribution function, produced by losses out of the atmospheric loss cones, as the most likely source of such free energy.

Based on the explicit calculation of quasilinear pitch angle diffusion coefficients using concurrently observed amplitudes of the $(3/2)f_{ce}$ and f_{UH} noise, the apparent absence of deep loss cones is also consistent with the expectation that these plasmas are on or near a state of strong pitch angle diffusion.

Acknowledgements

We wish to thank M. Ashour-Abdalla for numerous discussions during the course of this investigation, and C.T. Russell for access to the ISEE magnetic field measurements used in preparing Figures 1 and 2.

Research at the University of California was supported by the National Aeronautics and Space Administration Contract NAS5-20094 from the Goddard Space Flight Center under University of Iowa Subcontract R44855. The research at the University of Iowa was supported under NASA Contracts NAS5-20093 and NAS5-20094 from the Goddard Space Flight Center and Grant MGL-16-001-043.

References

Ashour-Abdalla, M., and C.F. Kennel, Convective cold upper hybrid instabilities, in *Magnetospheric Particles and Fields*, B.M. McCormac (ed.), pp. 181-196, D. Reidel, Dordrecht-Holland, 1976.

Ashour-Abdalla, M., and C.F. Kennel, Non-convective and convective electron cyclotron harmonic instabilities, *J. Geophys. Res.*, *83*, 1531-1543, 1978.

Christiansen, P.J., M.P. Gough, G. Martelli, J.J. Bloch, N. Cornilleau, J. Etcheto, R. Gendrin, C. Behin, P. Decreau, and D. Jones, GEOS-1 observations of electrostatic waves, and their relationship with plasma parameters, *Space Sci. Rev.*, *22*, 383-400, 1978.

Craven, J.D., and L.A. Frank, Electron angular distributions above the dayside auroral oval, *J. Geophys. Res.*, 81, 1695-1699, 1976.

Frank, L.A., D.M. Yeager, H.D. Owens, K.L. Ackerson, and M.R. English, Quadrispherical Lepedeas for ISEE-1 and -2 plasma measurements, *IEEE Trans. Geoscience Electronics*, GE-16, pp. 221-225, 1978a.

Frank, L.A., K.L. Ackerson, R.J. DeCoster, and B.G. Burek, Three-dimensional plasma measurements within the earth's magnetosphere, *Space Sci. Rev.*, *22*, 739-763, 1978b.

Gurnett, D.A., F.L. Scarf, R.W. Fredricks, and E.J. Smith, The ISEE-1 and ISEE-2 plasma wave investigation, *IEEE Trans. Geoscience Electronics*, GE-16, pp. 225-230, 1978.

Gurnett, D.A., R.R. Anderson, F.L. Scarf, R.W. Fredricks, and E.J. Smith, Initial results from the ISEE-1 and -2 plasma wave investigation, *Space Sci. Rev.*, 23, 103-122, 1979.

Hubbard, R.F., and T.J. Birmingham, Electrostatic emissions between electron gyroharmonics in the outer magnetosphere, *J. Geophys. Res.*, *83*, 4837-4850, 1978.

Hubbard, R.F., T.J. Birmingham and E.C. Hones, Magnetospheric electrostatic emissions and cold plasma densities, *J. Geophys. Res.* (in press), 1979.

Kennel, C.F., and F. Engelmann, Velocity space diffusion from weak plasma turbulence in a magnetic field, *Phys. Fluids*, *9*, 2377-2388, 1066.

Kennel, C. F., F. L. Scarf, R. W. Fredricks, J. H. McGehee, and F.V. Coroniti, VLF electric field observations in the magnetosphere, *J. Geophys. Res.*, 75, 6136, 1970.

Kurth, W.S., J.D. Craven, L.A. Frank, and D.A. Gurnett, Intense electrostatic waves near the upper hybrid resonance frequency, *J. Geophys. Res.*, (in press), 1979a.

Kurth, W.S., M. Ashour-Abdalla, L.A. Frank, C.F. Kennel, D.A, Gurnett, D.D. Sentman, and B.G. Burek, A comparison of intense electrostatic waves near f_{UHR} with linear instability theory, *Geophys. Res. Lett.*, *6*, 487, 1979b.

Lyons, L.R., Electron diffusion driven by magnetospheric electrostatic waves, *J. Geophys. Res.*, *79*, 575-580, 1974.

Rönnmark, K., H. Borg, P.J. Christiansen, M.P. Gough, and D. Jones, Banded electron cyclotron harmonic instability – a first comparison of theory and experiment, *Space Sci. Rev.*, 22, 401-417, 1978.

Scarf, F.L., R.W. Fredricks, C.F. Kennel, and F.V. Coroniti, Satellite studies of magnetospheric substorms on August 15, 1968. 8. OGO 5 plasma wave observations, *J. Geophys. Res.*, *78*, 3119-3130, 1973.

Schield, M.A., and L.A. Frank, Electron observations between the inner edge of the plasma sheet and the plasmasphere, *J. Geophys. Res.*, 75, 5401-5415, 1970.

Shaw, R.R., and D.A. Gurnett, Electrostatic noise bands associated with the electron gyrofrequency and plasma frequency in the outer magnetosphere, *J. Geophys. Res.*, *80*, 4259-4271, 1975.

Young, T.S., J.D. Callen, and J.E. McCune, High frequency electrostatic waves in the magnetosphere, *J. Geophys. Res.*, 78, 1082, 1973.

(Received July 23, 1979;
accepted August 22, 1979.)